1-1-2008

Microfluidic Delivery of Small Molecules into Mammalian Cells Based on Hydrodynamic Focusing

F Wang

H Wang

J Wang

H.-Y. Wang

P L. Rummel

See next page for additional authors

Wang, F; Wang, H; Wang, J; Wang, H.-Y.; Rummel, P L.; Garimella, S V.; and Lu, C, "Microfluidic Delivery of Small Molecules into Mammalian Cells Based on Hydrodynamic Focusing" (2008). *CTRC Research Publications.* Paper 97.
http://dx.doi.org/10.1002/bit.21737

Microfluidic Delivery of Small Molecules into Mammalian Cells Based on Hydrodynamic Focusing

Fen Wang [a], Hao Wang [b], Jun Wang [a], Hsiang-Yu Wang [c], Peter L. Rummel [a], Suresh V. Garimella [b] and Chang Lu *[acde]

[a] Department of Agricultural and Biological Engineering, [b] School of Mechanical Engineering, [c] School of Chemical Engineering, [d] Birck Nanotechnology Center, [e] Bindley Bioscience Center, Purdue University, West Lafayette, Indiana 47907, USA

*Corresponding author: Chang Lu, Department of Agricultural and Biological Engineering, 225 S. University Street, Purdue University, West Lafayette, IN 47907

Tel: (+1)765-494-1188

Fax: (+1)765-496-1115

Email: changlu@purdue.edu

Abstract

Microfluidics-based cell assays offer high levels of automation and integration, and allow multiple assays to be run in parallel, based on reduced sample volumes. These characteristics make them attractive for studies associated with drug discovery. Controlled delivery of drug molecules or other exogenous materials into cells is a critical issue that needs to be addressed before microfluidics can serve as a viable platform for drug screening and studies. In this study, we report the application of hydrodynamic focusing for controlled delivery of small molecules into cells immobilized on the substrate of a microfluidic device. We delivered calcein AM which was permeant to the cell membrane into cells, and monitored its enzymatic conversion into fluorescent calcein during and after the delivery. Different ratios of the sample flow to the side flow were tested to determine how the conditions of hydrodynamic focusing affected the delivery. A 3D numerical model was developed to help understand the fluid flow, molecular diffusion due to hydrodynamic focusing in the microfluidic channel. The results from the simulation indicated that the calcein AM concentration on the outer surface of a cell was determined by the conditions of hydrodynamic focusing. By comparing the results from the simulation with those from the experiment, we found that the calcein AM concentration on the cell outer surface correlated very well with the amount of the molecules delivered into the cell. This suggests that hydrodynamic focusing provides an effective way for potentially quantitative delivery of exogenous molecules into cells at the single cell or subcellular level. We expect that our technique will pave the way to high-throughput drug screening and delivery on a microfluidic platform.

Introduction

Microfluidics-based cell assays have been extensively explored for a wide range of applications including single cell analysis and measurement, microscale biophysics and biochemistry, and tissue engineering. [1, 2] Microfluidics not only provides the capability of microscale manipulation or confinement for isolation of single cells but also offers controlled microenvironments down to subcellular dimensions. [3-9] The introduction of a local perturbation to the subcellular area is critical for the continuous observation of effects of particular chemical/biological reagents on the biochemical and biophysical processes of cells and for the study of the propagation of these effects from a local area to the whole cell.[7-9] In these studies, the special characteristics related to microscale laminar flows have been explored for the local application of stimulants to a subcellular area. Together with the capability of subcellular delivery of reagents, other features offered by microfluidics, such as a high degree of integration, automation, and high throughput, make it a unique platform for a wide range of applications related to drug discovery and other cell biology studies related to cell stimulation and response. However, microfluidics has only been explored in limited cases for applications related to the delivery of chemical, drug molecules, or nanoparticles into cells. [5, 10-12] Microfluidic delivery of molecules into cells in a controlled and quantitative manner remains a challenge.

In this study, we demonstrate the delivery of small molecules into cells based on microfluidic hydrodynamic focusing. In hydrodynamic focusing, the side flows squeeze the central flow into a thin stream that is sheathed in buffer fluid. The combined streams flow in parallel down the channel with mixing between the streams caused only due to diffusion.

[13-15] The focusing width can be controlled by varying the ratio of relative pressure driving the side and central flows, and stream widths as small as 50 nm have been measured.[13] Hydrodynamic focusing has been applied to a number of different applications ranging from single molecule analysis[16], rapid mixing or dilution[15-17], and microscale patterning of the surface[18], to the fabrication of monodisperse particles or liposomes. [19, 20]

In this study, we combine experiments and modeling to demonstrate controlled delivery of a membrane-permeant dye, calcein AM, into Chinese hamster ovary (CHO-K1) cells based on hydrodynamic focusing. The cells were immobilized on the bottom surface of the channel. By controlling the focus width of the central sample flow, we were able to adjust the amount of small molecules delivered into the cells. Hydrodynamic focusing enabled delivery of molecules through the subcellular membrane area in a stable and controlled manner. We monitored the dynamics of the enzymatic reaction and molecular diffusion inside the cells following the delivery of the molecule. Our modeling showed that the response of a cell was correlated with the concentration of the molecules available on the outer surface of the cell. This delivery technique could provide the basis for high-throughput screening of small molecule drugs on a microfluidic platform.

Experiments and Simulation

Microchip fabrication. Microfluidic devices were fabricated in polydimethylsiloxane (PDMS) using standard soft lithography method. [21] The detailed procedures are described in our previous publications. [22, 23] Briefly, microscale patterns were first created using computer-aided design software and then printed out on high-resolution (5080 dpi)

transparencies. The transparencies were used as photomasks in photolithography on a negative photoresist (SU-8 2010, MicroChem Corp., Newton, MA). The thickness of the photoresist and hence the depth of the channels was around 33 μm (measured by a Sloan Dektak3 ST profilometer). The pattern of channels in the photomask was replicated in SU-8 after exposure and development. The microfluidic channels were molded by casting a layer (~5 mm) of PDMS prepolymer mixture (General Electric Silicones RTV 615, MG Chemicals, Toronto, Ontario, Canada) with a mass ratio of A:B=10:1 on the photoresist/silicon wafer master treated with tridecafluoro-1,1,2,2-tetrahydrooctyl-1-trichlorosilane (United Chemical Technologies, Bristol, PA). The prepolymer mixture was cured at 80°C for 30 minutes in an oven and then peeled off from the maser. The PDMS chip was sealed to 1 mm thick, 1×3 inch glass slides by oxidation using a Tesla coil (Kimble/Kontes, Vineland, NJ) in atmosphere, immediately before use. The PDMS chip and the glass slide were sterilized by exposing to UV light overnight in a tissue culture hood before bonding and use. [24]

General cell culture. Chinese hamster ovary (CHO-K1) cells were cultured in plastic tissue culture flasks at 37°C, under 5% CO_2 in Dulbecco's modified Eagle's medium (DMEM, Mediatech Inc., Herndon, VA) supplemented with 10% (v/v) fetal bovine serum (FBS, Sigma, St. Louis, MO), penicillin (100 units/ml, Sigma, St. Louis, MO), and streptomycin (100μg/ml, Sigma, St. Louis, MO). Cells were diluted at a ratio of 1:5 every 3 days to maintain them in the exponential growth phase (~1×10^6 cells/ml). They were harvested by adding Trypsin-EDTA (Sigma, St. Louis, MO) to the culture and centrifuged at 300g for 10 minutes to remove the supernatant. The cells were then resuspended in the

culture medium at a concentration of 1×10^6 cells/ml for seeding in the microfluidic device.

Cell seeding and culture in the microfluidic device. All the procedures related to the cell seeding and culture in the microfluidic device were carried out inside a Class II type A2 biological safety cabinet. The channels were coated with fibronectin from bovine plasma (Sigma, St. Louis, MO) to facilitate cell adhesion. Fibronectin is a glycoprotein which interacts with the cell surface receptor or extracellular matrix to mediate cell adhesion. Fibronectin was prepared at a concentration of 100 μg/ml in PBS (Sigma, St. Louis, MO) before each experiment, and then flowed into the microfluidic device and incubated at 37°C for 1 hour. CHO-K1 cells were suspended in the culture media at 1×10^6 cells/ml and loaded into the sample reservoir of the microfluidic device. The cells in the media readily flowed into the central channel under gravity due to the liquid level in the reservoir. The media level in the other two inlet reservoirs (connected the side channels) kept the cells from getting into the side channels. Cells were able to attach to the coated surface typically within 10 minutes. After adding extra culture media in the three inlet and one outlet reservoirs with the liquid level about the same, the device with seeded cells was transferred to a 37°C, 5% CO_2 incubator for 12 hours before the hydrodynamic focusing experiments involving cells. We found that renewing the media in the reservoirs every 3-4 hours provided enough media to support cell growth inside the device.

Phase contrast and fluorescence microscopy. During the hydrodynamic focusing delivery experiments, we observed the cells in the channel using a fluorescence microscope (IX-71, Olympus, Melville, NY) with a 40X dry objective (NA=0.40). The epifluorescence excitation was provided by a 100W mercury lamp, together with brightfield illumination

and a phase contrast condenser. The excitation and emission from cells loaded with calcein AM were filtered by a fluorescence filter cube (exciter HQ480/40, emitter HQ535/50, and beamsplitter Q505lp, Chroma technology, Rockingham, VT). The images of the cells were taken with a CCD camera (ORCA-285, Hamamatsu, Bridgewater, NJ). Great care was exercised to decrease photobleaching due to excessive exposure. The shutter was opened for less than 3 seconds each time to take a single image. The settings for the CCD camera and the software were kept identical from one experiment to another when comparison between experiments was desired.

Preparation of fluorescent dye solutions. To observe the hydrodynamic focusing in the microfluidic device, fluorescein ($C_{20}H_{12}O_5$, Sigma, St. Louis, MO) was prepared at a concentration of 2 mM in 1M NaOH solution which resulted in the strongest emission. Calcein AM (MW = 995), a cell permeant dye (Molecular Probes, Eugene, OR),was stored in high-quality, anhydrous dimethysulfoxide (DMSO), and diluted to 20 μg/ml in PBS buffer before delivery experiments.

Microchip operation for delivery of calcein AM into cells. For the delivery experiments, the setup and the configuration of the device are shown in Figure 1. All the channels are 100 μm wide and 33 μm deep. The culture medium in the channels (with seeded cells) was removed and flushed twice with PBS buffer. To apply accurate flow rate control, the two side channels of the device were connected to a syringe pump (PHD infusion pump, Harvard Apparatus, Holliston, MA), whereas the central sample inlet was connected to a second syringe pump of the same model. The syringes and the plumbing components were sterilized by washing with 70% (v/v) ethyl alcohol before each experiment. The central

sample inlet with a flow rate set at 30 μl/hr delivered calcein AM with a concentration of 20 μg/ml. PBS buffer flowed into the two side channels (with both channels experiencing the same flow rate) to squeeze the sample flow to a certain focus width. The ratio of the flow rate in either side channel to that in the central channel ranged from 3 to 20. In a typical experiment, calcein AM delivery (under hydrodynamic focusing) lasted for a period of time before being stopped. The flow of PBS buffer into the side channels was continued to remove the extra calcein AM.

Simulation of hydrodynamic focusing and molecular diffusion

The steady state fluid flow and molecular diffusion within the microfluidic device were simulated using the commercial finite volume software FLUENT 6 (Fluent Inc., Lebanon, NH, USA). A 3-D model was generated with the same dimensions as those of the device employed in the experiments (channels of 100 μm width and 33 μm depth as in Figure 1).

Considering the small scale and slow velocities, the flow was modeled as being incompressible and laminar, using the continuity and momentum equations as follows:

$$\nabla \cdot \vec{V} = 0 \qquad (1)$$

$$0 = -\nabla p + \nabla \cdot (\mu \nabla \vec{V}) \qquad (2)$$

The species equation for Calcein AM diffusion is:

$$0 = -\vec{V}\nabla(\rho F) + \nabla \cdot (\rho D \nabla F) \qquad (3)$$

In these equations, ρ [kg/m^3] and μ [$Pa.s$] are the density and dynamic viscosity of the dye solution which is approximated with the properties for water, V [m/s] is the flow velocity, P [Pa] is the dynamic pressure, F is the mass fraction of the dye, and D [m^2/s] is the diffusion coefficient of the dye molecule.

Second-order upwind differencing was applied in discretizing the advection terms, while the SIMPLE algorithm was employed for pressure–velocity coupling.[25] The boundary condition at the inlet of the three channels was set as a velocity-inlet boundary since the inlet velocity was known; the bulk flow velocity for the central channel was set as 2.53 mm/s (30 μl/hr) and the velocities for the side channels were related to this value via the flow rate ratio *k*. The boundary condition at the outlet was set as a given static pressure outlet. [26] At the channel walls, a no-slip boundary condition was applied. The dye concentration at the inlet of the central channel was set as 20 μg/ml, while that at the inlet of the two side channels was set as 0.

Results and Discussion

Hydrodynamic focusing of fluorescein in the microfluidic device

We applied a fluorescent dye (fluorescein) to visualize the hydrodynamic focusing in the microfluidic device in the absence of cells. The focusing within 450 μm from the intersection was observed. The effect of the flow rate ratio *k* between the side flow (containing the neat buffer) and the central flow (containing the sample of small molecules) on the focus width was studied in the experiment, with the central channel flow rate kept constant. The ratio of the side flow rate to the sample flow rate was defined as

$$k = \frac{V_{side}}{V_{central}} \qquad (4)$$

in which V_{side} and $V_{central}$ are the volumetric flow rates in either of the two side channels and in the central channel, respectively. The images of hydrodynamic focusing of fluorescein under different flow rate ratios are shown in Figure 2a. The focus widths of fluorescein

along the channel length (we designated the left boundary of the vertical channel as x = 0) are plotted in Figure 2b. Fluorescein has a molecular weight of 332 and an estimated diffusion coefficient of 3.8×10^{-10} m^2/s. [27, 28] It may be noted that the focus width observed with the CCD camera is dependent on the sensitivity and the dynamic range of the CCD camera. In general the focus width decreased when the flow rate ratio k increased. The focus widths were fairly constant for x in the range of 200 and 350 μm. When the flow rate ratio k was 10 or higher, the focus width was less than 10 μm. This suggests that streams carrying small molecules with subcellular dimensions can be easily created using this approach.

Calcein AM delivery and conversion in the seeded cells

Calcein AM is a neutral and non-fluorescent dye that is permeant to the cell membrane. Once the dye enters a cell, it is rapidly converted by cell esterases into negatively charged, impermeant fluorescent molecules (calcein).[29] The nucleus-cytoplasm signal intensity ratio is approximately 3:1, which allows clear visualization of both structures. In this study, we used calcein AM as a model molecule to test the controlled delivery of small molecules into cells based on microfluidic hydrodynamic focusing.

After growing cells on the surface of the glass substrate for 12 hours, we tested the delivery of calcein AM by flowing the sample stream (20 μg/ml calcein AM in PBS buffer) under hydrodynamic focusing from the two side flows (PBS buffer). Since calcein AM is not fluorescent, the focus width of the central sample stream could not be directly observed. Due to the similar diffusion coefficients of calcein AM and fluorescein (estimated as 2.6×10^{-10} and 3.8×10^{-10} m^2/s, respectively), we assumed that the focusing of calcein AM was

similar to that of fluorescein. [27, 28] Figure 3 confirms that when the flow rate ratio *k* was 5 with the inlet sample flow rate of 30 μl/hr, only the cells along the center of the channel were labeled after flowing calcein AM for 5 minutes. Based on our experiments with fluorescein (Figure 2), the focus width in this case is expected to be approximately 15 μm.

Figure 4 shows the entire process of the delivery and conversion of calcein AM using our technique. A single CHO-K1 cell was monitored during delivery of calcein AM at a flow rate ratio k of 20 for the initial 25 minutes. The fluorescence first appeared in the nucleus although the delivery of the dye was to the periphery of the cell based on its location in the channel. This was presumably determined by the local concentration of esterases inside the cell. The fluorescence intensity reached a maximum shortly after the termination of the infusion of calcein AM and the intensity gradually declined thereafter. The decline in the fluorescence after 30 minutes is likely due to photobleaching over time (a fluorescence image was taken at the end of every minute by exposing the cells to a mercury lamp for a couple of seconds) and calcein leaking out of the cell.

Results from the delivery experiments carried out at varying flow rate ratios (k = 3, 5, 10, and 20) with the same central sample flow rate (30 μl/hr) are shown in Figure 5. Each curve represents an average of signals from 3 to 7 cells in the same region (x = 250~450 μm). A control experiment was also conducted by delivering calcein AM solution at 30 μl/hr in a straight channel (single-inlet single-outlet) without focusing. The delivery time of calcein AM was 5 minutes for each experiment, after which the calcein AM was removed with a stream of PBS buffer.

A higher flow rate ratio k yielded lower fluorescence intensity, implying that fewer

calcein AM molecules were delivered into the cells. The fluorescence intensity typically reached its peak value within 1 to 5 minutes after delivery of the calcein AM solution was stopped. When the flow rate ratio was lower and the concentration of calcein AM was higher around the cells, the peak value in the fluorescence intensity occurred later due to the time required for enzymatic processing of the molecules. The control experiment delivered more calcein AM into cells than all the experiments with hydrodynamic focusing. The peak value in the fluorescence intensity was indicative of the amount of calcein AM molecules delivered into cells.

It must be noted that our technique is fundamentally different from other hydrodynamics techniques such as "PARTCELL" in terms of the motivation and the application [7-9]. In this work, we are interested in developing a technique which is capable of delivering a tiny amount of molecules into single cells in a controlled manner. We are not interested in observing the effects of delivery into specific subcellular regions. Indeed, since the enzymatic conversion of calcein AM occurs mostly in the nucleus regardless of the delivery location (as shown in Figure 4), we do not expect to see significant effects due to the subcellular location where the delivery takes place. We are primarily concerned with how the dimensions of the carrier stream (which determine how much the membrane surface is exposed to the carrier stream) affect the amount of the molecules delivered to the whole cell.

Simulation of the hydrodynamic focusing and the molecular diffusion

Three-dimensional simulations of the flow field in the microfluidic device have been carried out to generate insight into how hydrodynamic focusing can be used to manipulate

the molecular delivery into a cell. However, the delivery of small molecules into cells, which is often followed by chemical or biological reactions inside the cells, can be a complicated process. The main difficulty with modeling the process is that there are no data in the literature on the properties associated with the diffusion, partition, and reaction of the molecule at the cell membrane interface and inside the cell. In this study, our approach is to focus on what occurs outside the cell. To simplify the situation, we assume that the calcein AM concentration in the microfluidic channel is not affected by the uptake of the molecule into cells since the solution flows by rapidly and the adsorbed molecules only account for a tiny fraction of the total amount. The focus of the analysis is then on molecular diffusion in the vicinity of a single cell under hydrodynamic focusing, which is approximated to have the shape of a half-ellipsoid (20, 60, and 5 μm in x, y, z direction, respectively, as shown in the inset of Figure 6b) is positioned at x = 300 μm with its length perpendicular to the flow direction. Since the concentration profile on the outer surface of the cell will set the boundary conditions for the delivery and reaction across the membrane and inside the cell, we expect the concentration profile to be strongly correlated with the amount of the molecules delivered.

Figure 6 shows the mesh of the 3D model and the dimensions and position of the cell. A mesh with 128,333 hexahedral elements was found to yield mesh-independent results, and was chosen for the simulations.

Figure 7 shows the simulation results for the concentration field of calcein AM under flow rate ratios 3, 5, 10, and 20 with a single cell seeded in the channel. Calcein AM is not fluorescent (it only becomes fluorescent when it is processed inside the cell and converted

to calcein) so that direct observation of its focusing using experimental methods is difficult. Instead, as mentioned earlier, the experimental results of fluorescein provide an estimate of the calcein AM focusing in view of the similarity in diffusion coefficients of these two molecules. In Figure 2 when $k = 3$, the focus width recorded by the CCD camera was approximately 20 μm at $x = 200$ μm. The simulated results for concentration distribution at $x = 200$ μm at the same flow rate ratio are shown in Figure 8a. Very good agreement is seen between the simulation results for calcein AM focusing (Figure 8b) and the experimental results of fluorescein focusing (Figure 2). The simulation shows that the presence of the cell does not substantially affect the concentration field and hydrodynamic focusing.

We further investigated the concentration gradient in the channel due to hydrodynamic focusing and diffusion. Figure 9 shows the calcein AM concentration distribution in the cross section of the channel in the ZY plane which intersects the center of the cell. The molecular profile slightly expands on the cell surface and the upper wall of the channel. The higher the flow rate ratio, the lower is the concentration in general.

Figure 10a shows the concentration of calcein AM on the outer surface of the cell in the XY plane. The calcein AM concentration is plotted along the Y axis (y = 0 at the cell center) in Figure 10b under different flow rate ratios. The concentration is the highest at the cell center. The peak concentration is around 16 μg/ml when k = 3 (compared to the original calcein AM concentration of 20 μg/ml). The magnitude of the peak concentration is seen to decrease as the flow rate ratio increases. We consider two competing mechanisms which determine the peak concentration on the cell surface: First, higher flow rates from the side channels squeeze the sample flow into a narrower stream so that the calcein AM

concentration in the central stream is lowered more rapidly due to the shorter diffusion length involved; second, a higher flow rate ratio is associated with higher overall velocity in the channel which shortens the time for the sample to reach the cell location. This decreases the time for diffusion to occur. The first mechanism seems to dominate for all the flow rate ratios explored in this study.

Lastly, we wished to determine whether the concentration on the outer surface of the cell affects the uptake of the molecule in a significant way. The peak values in the fluorescence intensity from cells after the delivery (Figure 5) indicated the number of calcein AM molecules delivered. The data in Figure 5 were extracted from multiple cells with different positions and orientations in the region of x = 250-450 μm, compared to the simulation in which a single cell at x = 300 μm was modeled. Nevertheless, the presence of cells does not seem to affect the hydrodynamic focusing in a significant way as we concluded above. Furthermore, the uptake of the molecule is essentially determined only by the surface area exposed to the carrier stream with the cell orientation being less relevant. In Figure 11, at each flow rate ratio, the averaged calcein AM concentration over the entire outer surface of the cell (obtained from the simulation) was plotted against the peak value in the fluorescence intensity after the delivery (obtained from the experiment). The two sets are seen to correlate very well. The Pearson's correlation coefficient r of 0.99 for this linear fit indicates that the number of molecules delivered into the cells has a strong linear correlation with the averaged concentration of calcein AM on the cell surface. This validates the effectiveness of our simulations. Since the concentration on the cell surface can be adjusted by hydrodynamic focusing, this in turn suggests that microfluidic

hydrodynamic focusing can effectively influence the number of the molecules delivered into cells.

Conclusions

In this study, we explored the possibility of applying microfluidic hydrodynamic focusing for controlled delivery of molecules into cells at the single cell or subcellular level. Combining experiments and simulations, we demonstrated that we were able to create a focused stream with a controlled flow rate and microscale width by hydrodynamic focusing. The focused stream delivered molecules into cells by flowing across the surface of cells adhering to the channel substrate. By controlling the focus width and the flow rate of the delivery stream, we were able to control how much the small molecules (calcein AM) were delivered. We envision that such a technique can form the basis for future drug screening based on microfluidics. By controlling the delivery quantitatively, our technique also presents the potential for mechanistic studies of the uptake and biochemical reactions in the cell.

Acknowledgements

We acknowledge Purdue University and Purdue Research Foundation for supporting this research.

References

(1) Breslauer, D.; Lee, P.; Lee, L. *Mol. Biosyst.* **2006,** *2*, 97-112.

(2) Andersson, H.; van den Berg, A. *Sens. Actuators B* **2003,** *92*, 315-325.

(3) Wu, H.; Wheeler, A.; Zare, R. *Proc. Natl. Acad. Sci. U.S.A.* **2004,** *101*, 12809-12813.

(4) Sabounchi, P.; Ionescu-Zanetti, C.; Chen, R.; Karandikar, M.; Seo, J.; Lee, L. *Appl. Phys. Lett.* **2006,** *88*, 183901.

(5) Werdich, A.; Lima, E.; Ivanov, B.; Ges, I.; Anderson, M.; Wikswo, J.; Baudenbacher, F. *Lab Chip* **2004,** *4*, 357-362.

(6) Lucchetta, E.; Lee, J.; Fu, L.; Patel, N.; Ismagilov, R. *Nature* **2005,** *434*, 1134-1138.

(7) Takayama, S.; Ostuni, E.; LeDuc, P.; Naruse, K.; Ingber, D.; Whitesides, G. *Chem. Biol.* **2003,** *10*, 123-130.

(8) Takayama, S.; Ostuni, E.; LeDuc, P.; Naruse, K.; Ingber, D.; Whitesides, G. *Nature* **2001,** *411*, 1016-1016.

(9) Sawano, A.; Takayama, S.; Matsuda, M.; Miyawaki, A. *Dev. Cell* **2002,** *3*, 245-257.

(10) Davidsson, R.; Boketoft, A.; Bristulf, J.; Kotarsky, K.; Olde, B.; Owman, C.; Bengtsson, M.; Laurell, T.; Emneus, J. *Anal. Chem.* **2004,** *76*, 4715-4720.

(11) Kraus, T.; Verpoorte, E.; Linder, V.; Franks, W.; Hierlemann, A.; Heer, F.; Hafizovic, S.; Fujii, T.; de Rooij, N. F.; Koster, S. *Lab Chip* **2006,** *6*, 218-29.

(12) Farokhzad, O. C.; Khademhosseini, A.; Jon, S.; Hermmann, A.; Cheng, J.; Chin, C.; Kiselyuk, A.; Teply, B.; Eng, G.; Langer, R. *Anal. Chem.* **2005,** *77*, 5453-9.

(13) Knight, J.; Vishwanath, A.; Brody, J.; Austin, R. *Phys. Rev. Lett.* **1998,** *80*, 3863-3866.

(14) Stiles, T.; Fallon, R.; Vestad, T.; Oakey, J.; Marr, D.; Squier, J.; Jimenez, R. *Microfluid. Nanofluid.* **2005,** *1*, 280-283.

(15) Pollack, L.; Tate, M. W.; Darnton, N. C.; Knight, J. B.; Gruner, S. M.; Eaton, W. A.;

Austin, R. H. *Proc. Natl. Acad. Sci. U.S.A.* **1999,** *96*, 10115-7.

(16) Lipman, E. A.; Schuler, B.; Bakajin, O.; Eaton, W. A. *Science* **2003,** *301*, 1233-5.

(17) Bousse, L.; Mouradian, S.; Minalla, A.; Yee, H.; Williams, K.; Dubrow, R. *Anal. Chem.* **2001,** *73*, 1207-1212.

(18) Regenberg, B.; Kruhne, U.; Beyer, M.; Pedersen, L.; Simon, M.; Thomas, O.; Nielsen, J.; Ahl, T. *Lab Chip* **2004,** *4*, 654-657.

(19) Xu, S.; Nie, Z.; Seo, M.; Lewis, P.; Kumacheva, E.; Stone, H.; Garstecki, P.; Weibel, D.; Gitlin, I.; Whitesides, G. *Angew. Chem. Int. Ed.* **2005,** *44*, 724-728.

(20) Jahn, A.; Vreeland, W.; Gaitan, M.; Locascio, L. *J. Am. Chem. Soc.* **2004,** *126*, 2674-2675.

(21) Duffy, D.; McDonald, J.; Schueller, O.; Whitesides, G. *Anal. Chem.* **1998,** *70*, 4974-4984.

(22) Wang, H. Y.; Lu, C. *Biotechnol. Bioeng.* **2006,** *95*, 1116-1125.

(23) Wang, H. Y.; Lu, C. *Anal. Chem.* **2006,** *78*, 5158-5164.

(24) Yu, H.; Meyvantsson, I.; Shkel, I.; Beebe, D. *Lab Chip* **2005,** *5*, 1089-1095.

(25) Patankar, S. V., *Numerical heat transfer and fluid flow*.; Hemisphere: Washington, DC, 1980.

(26) Mathur, S. R.; Murthy, J. Y. *Numer. Heat Transfer, Part B* **1997,** *32*, 283-298.

(27) Hayduk, W.; Laudie, H. *AICHE J.* **1974,** *20*, 611-615.

(28) Lyman, W. J.; Reehl, W. F.; Rosenblatt, D. H., *Handbook of chemical property estimation methods: environmental behavior of organic compounds*; McGraw-Hill: New York, 1982.

(29) Gatti, R.; Belletti, S.; Orlandini, G.; Bussolati, O.; Dall'Asta, V.; Gazzola, G. *J. Histochem. Cytochem.* **1998,** *46*, 895-900.

Figure Captions

Figure 1 Schematic diagram of the microfluidic device for testing delivery of small molecules into cells. The stream carrying the small molecule flows in the central channel and PBS buffer flows in the two side channels for focusing. The cells adhere to the glass substrate in the channel downstream from the intersection. The width and depth of the channels was 100 μm and 33 μm, respectively. The inset shows a microscope image of the cells on the glass surface after seeding for 12 hours.

Figure 2 (a) Hydrodynamic focusing of fluorescein molecules. The flow rate ratio ($k = V_{side}/V_{central}$) took values of 20, 10, 5 and 3 with $V_{central}$ fixed at 30 μl/hr in the images from the top to the bottom. **(b)** The focus width of fluorescein molecules along the X axis under different flow rate ratios with $V_{central}$ at 30 μl/hr. (x = 0 at the left boundary of the vertical channel).

Figure 3 The fluorescent image **(a)** and phase contrast image **(b)** of seeded cells (x = 250-450 μm) after hydrodynamic focused delivery of calcein AM for 5 minutes under the flow rate ratio *k* of 5 and the inlet sample flow rate of 30 μl/hr.

Figure 4 The overlay phase contrast/fluorescent images of the cell (located at $x \approx 350$ μm)

during the process of calcein AM delivery. The flow of calcein AM (k = 20 and inlet sample flow rate = 30 μl/hr) was terminated at 25 minutes. **(a)** before the delivery; and **(b)** 10 minutes; **(c)** 15 minutes; **(d)** 20 minutes; **(e)** 30 minutes; **(f)** 40 minutes; and **(g)** 70 minutes after the delivery started.

Figure 5 The dynamics over time in the fluorescence intensity of the cells loaded with calcein AM under different flow rate ratios. All the experiments were done by loading cells with calcein AM for 5 minutes. Each curve was the average of 3~7 cells in the region of x = 250-450 μm.

Figure 6 (a) Mesh of the 3-D model used to study molecular diffusion within the microfluidic device. A cell of the shape of half an ellipsoid was positioned at x = 300 μm. **(b)** The dimensions and the position of the cell and the dimensions of the microfluidic device (same as those of the actual device).

Figure 7 Simulation of the hydrodynamic focusing of calcein AM molecules. The flow rate ratio ($k = V_{side}/V_{central}$) ranged from 3 to 20 with $V_{central}$ (calcein AM carrying stream) being held at 30 μl/hr. The numbers on the scale bar are in units of μg/ml.

Figure 8 (a) The determination of the focus width based on the simulated concentration profile along the Y axis (x = 200 μm, z = 16.5 μm). The profile at flow rate ratio of 3 is used as an example and 0.6 μg/ml is designated as the threshold value for detection in

comparisons with experimental results. **(b)** The simulated focus widths of calcein AM molecules along the x axis under different flow rate ratios with $V_{central}$ at 30 μl/hr. The simulation shows good quantitative agreement with the experimental data in Figure 2b.

Figure 9 Simulated concentration distribution of calcein AM in the cross section of the channel (YZ plane) above the cell under different flow rate ratios with $V_{central}$ at 30 μl/hr. The numbers on the scale bar are in units of μg/ml.

Figure 10 (a) Simulated concentration of calcein AM on the cell surface under different flow rate ratios with $V_{central}$ at 30 μl/hr. The numbers on the scale bar are in units of μg/ml. **(b)** The calcein AM concentration on the cell surface plotted along the Y axis at x = 300 μm under different flow rate ratios (Y = 0 at the cell center).

Figure 11 The correlation between the average calcein AM concentration on the cell surface (simulated) and the peak fluorescence intensity after calcein AM delivery (experimental). The fluorescence intensity data were the average generated by a group of 3~7 cells in the region of x = 250-450 μm. The Pearson's correlation coefficient is $r = 0.99$.

Figures

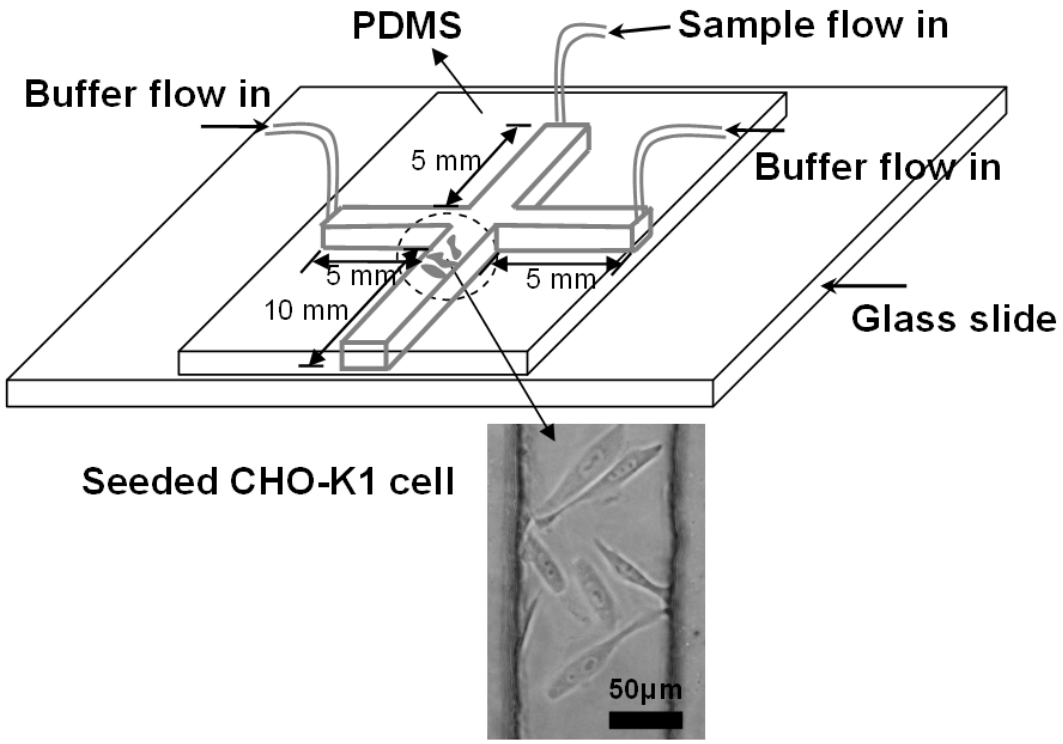

Figure 1

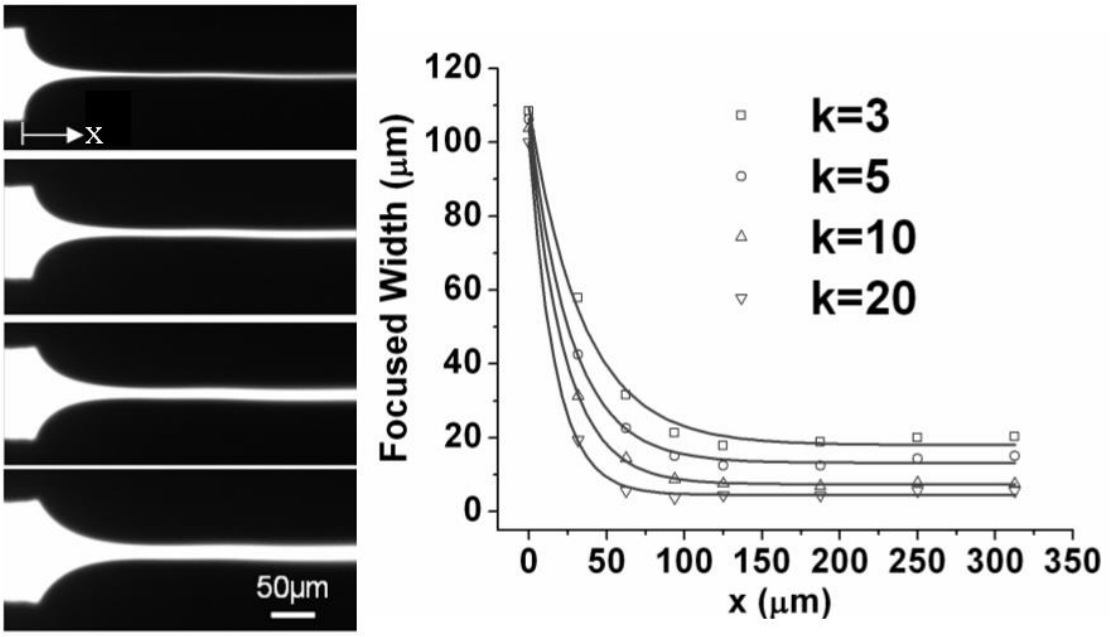
x
50μm
Focused Width (μm)
120
100
80
60
40
20
0
0
50
100
150
200
250
300
350
x (μm)
k=3
k=5
k=10
k=20

(a) (b)

Figure 2

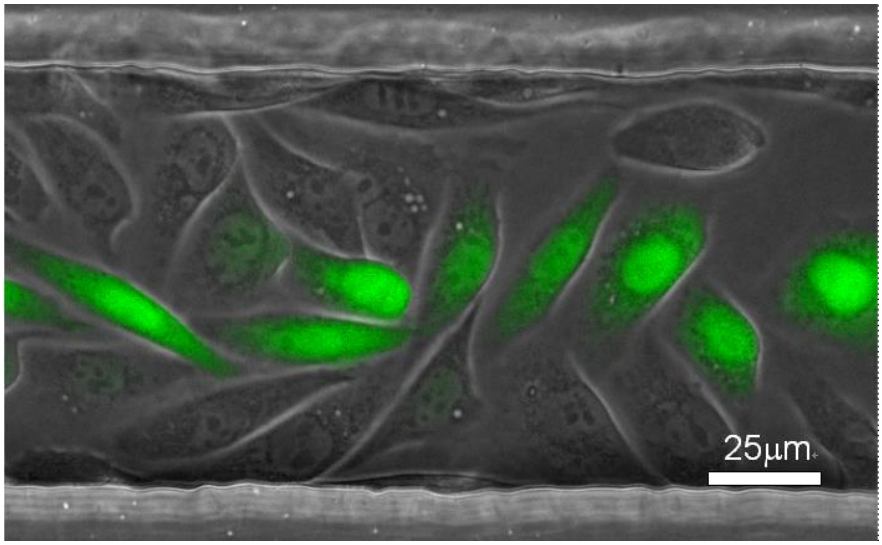

Figure 3

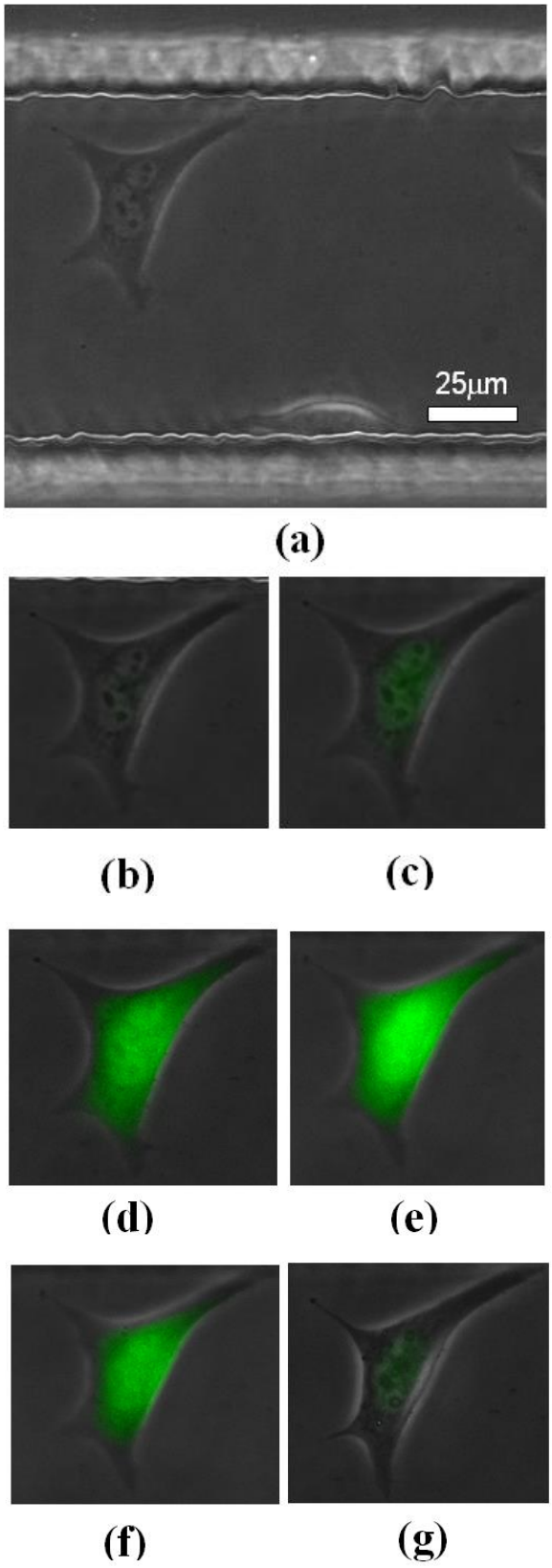

Figure 4

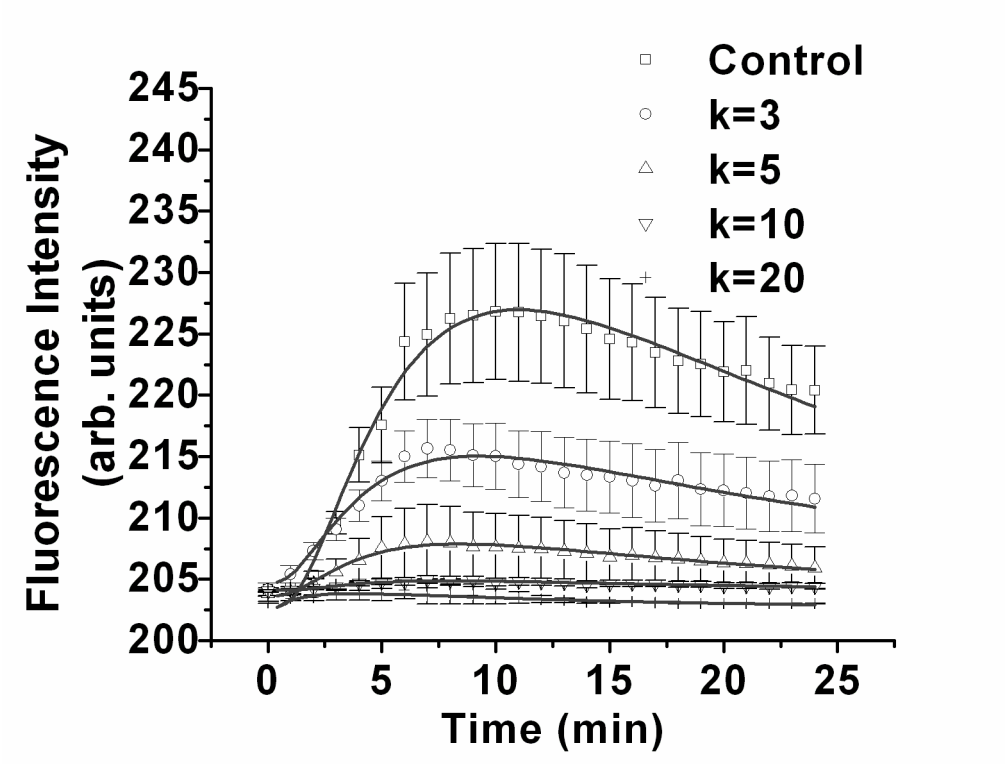
Control
k=3
k=5
k=10
k=20
Fluorescence Intensity
(arb. units)
245
240
235
230
225
220
215
210
205
200
0
5
10
15
20
25
Time (min)

Figure 5

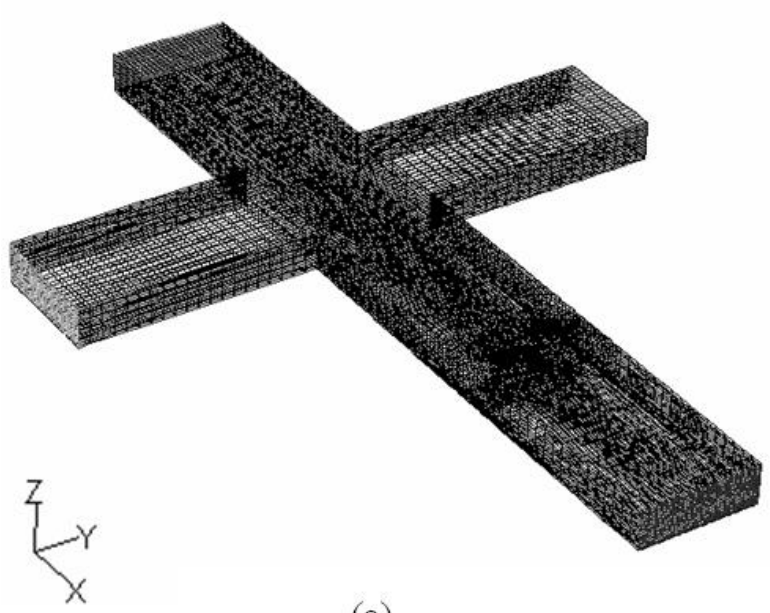

(a)

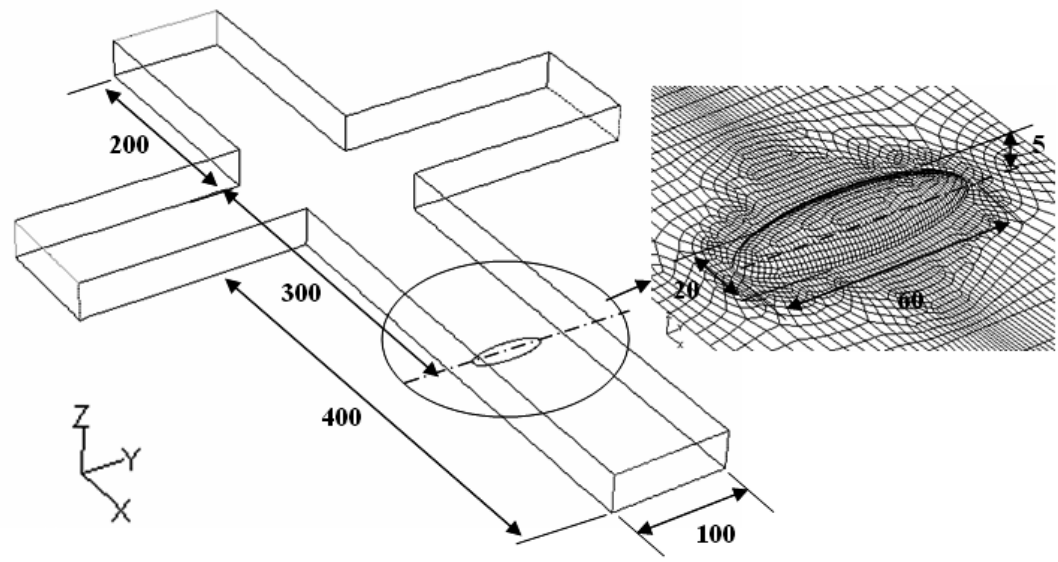

(b)

Figure 6

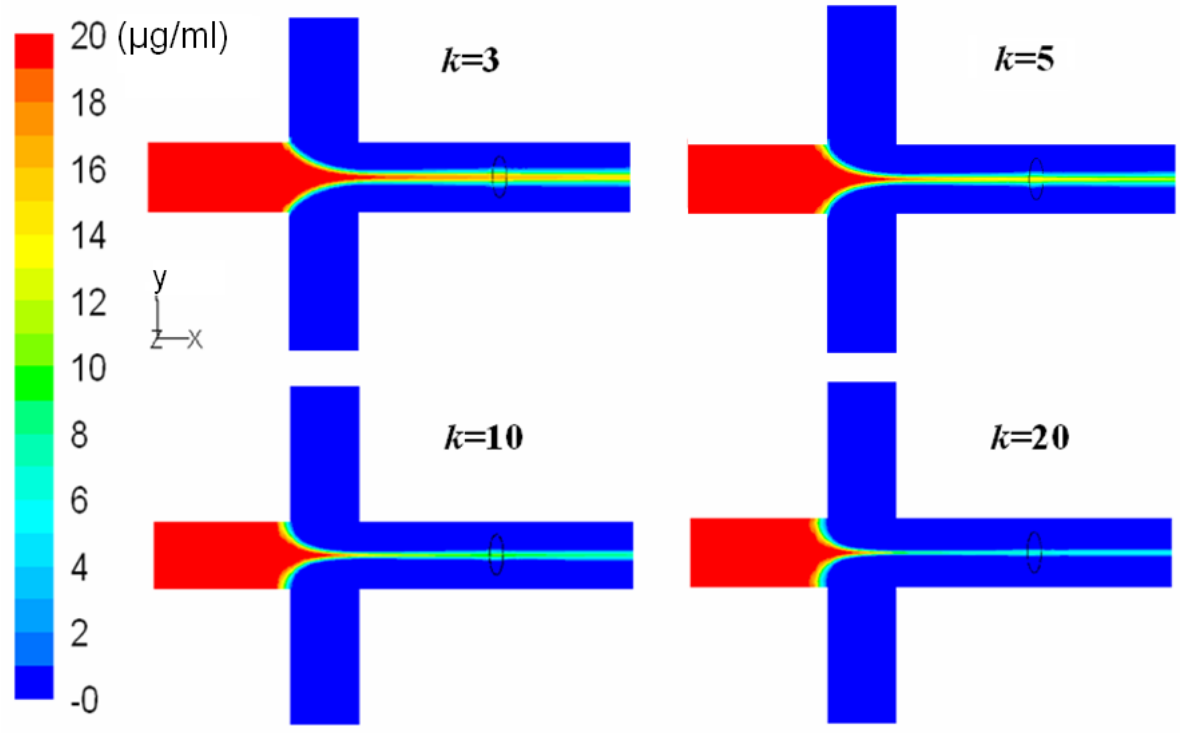

Figure 7

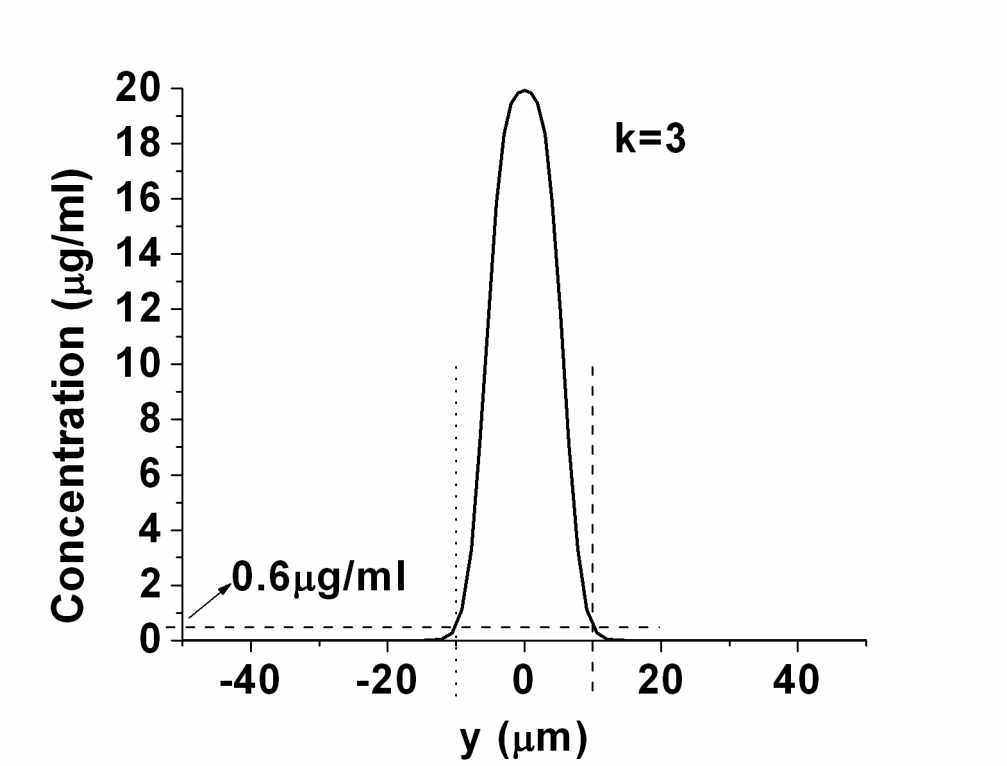
Concentration (μg/ml)
y (μm)
k=3
0.6μg/ml
20
18
16
14
12
10
8
6
4
2
0
-40
-20
0
20
40

(a)

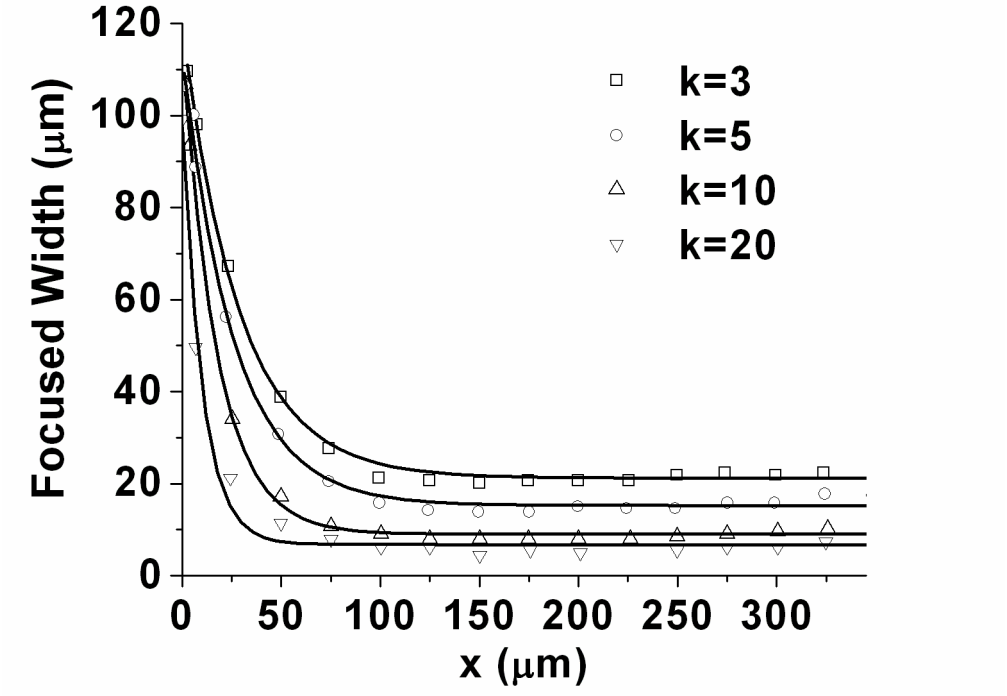
Focused Width (μm)
x (μm)
k=3
k=5
k=10
k=20
120
100
80
60
40
20
0
0
50
100
150
200
250
300

(b)

Figure 8

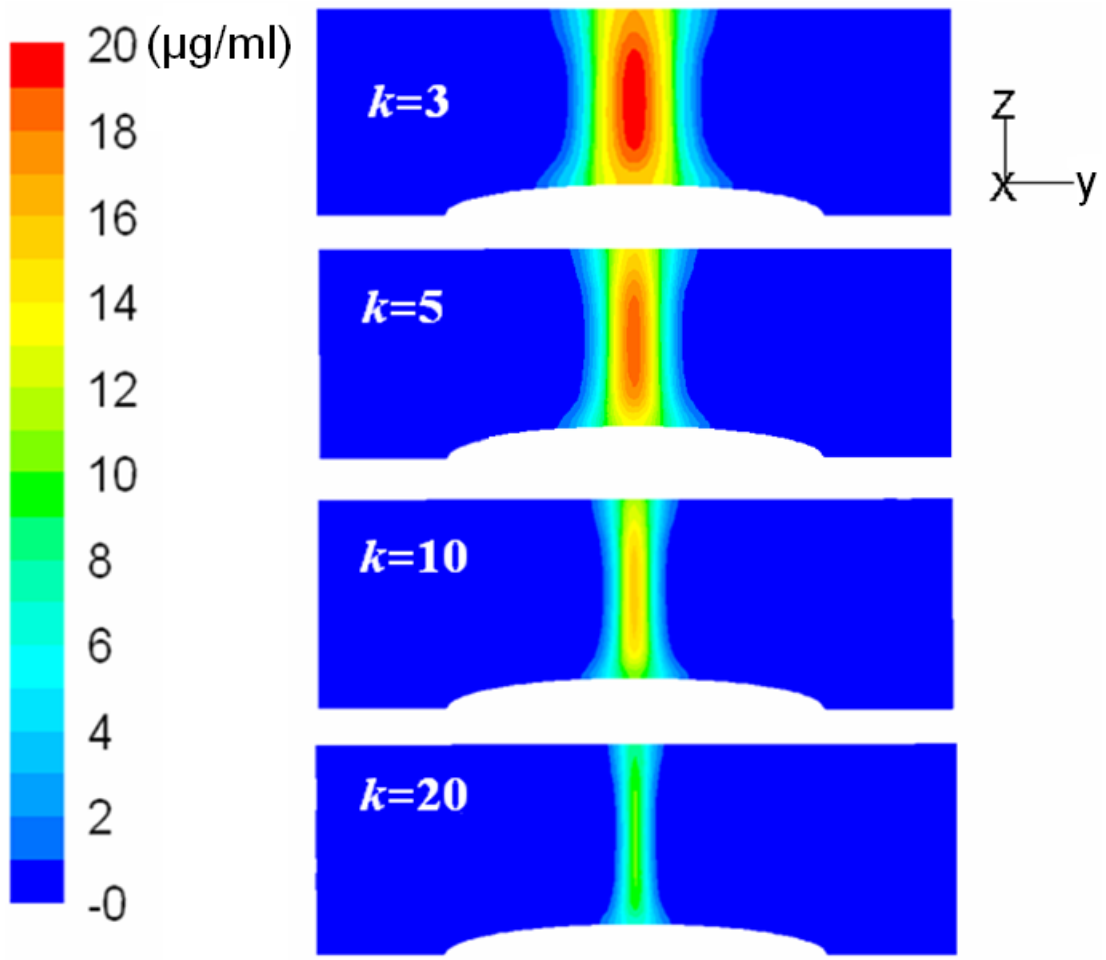

Figure 9

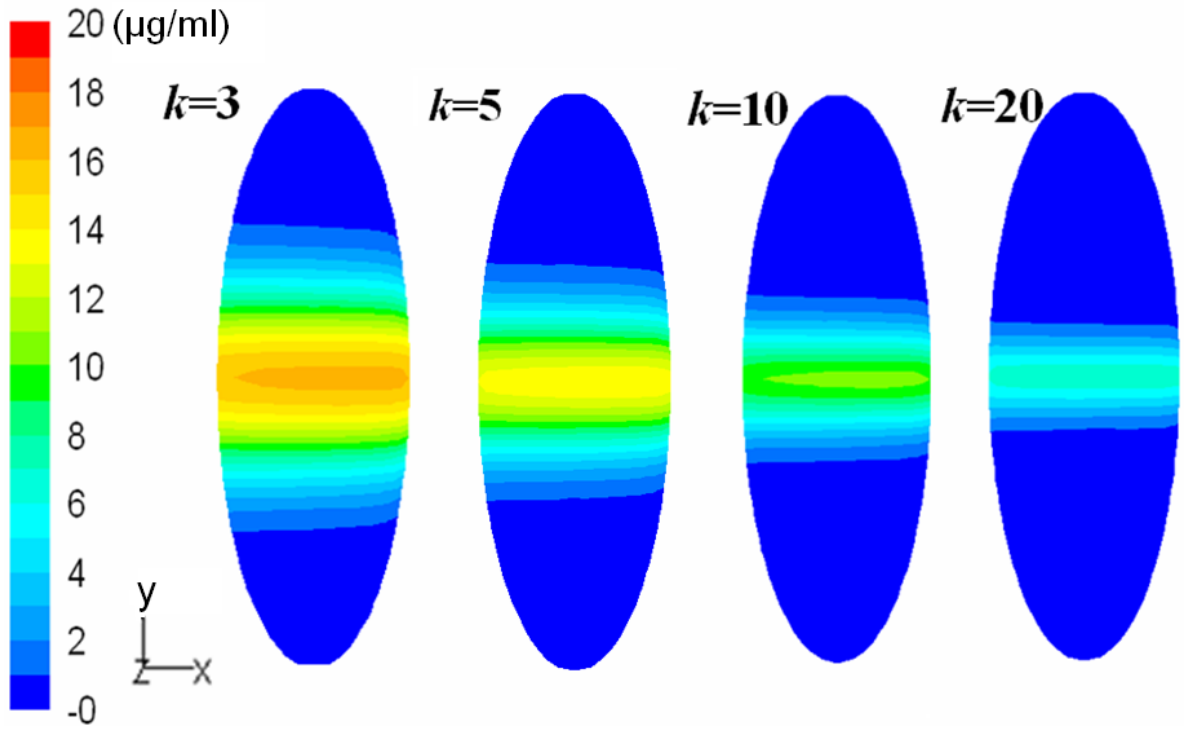
20 (μg/ml)
18
16
14
12
10
8
6
4
2
-0
k=3
k=5
k=10
k=20
y
z
x

(a)

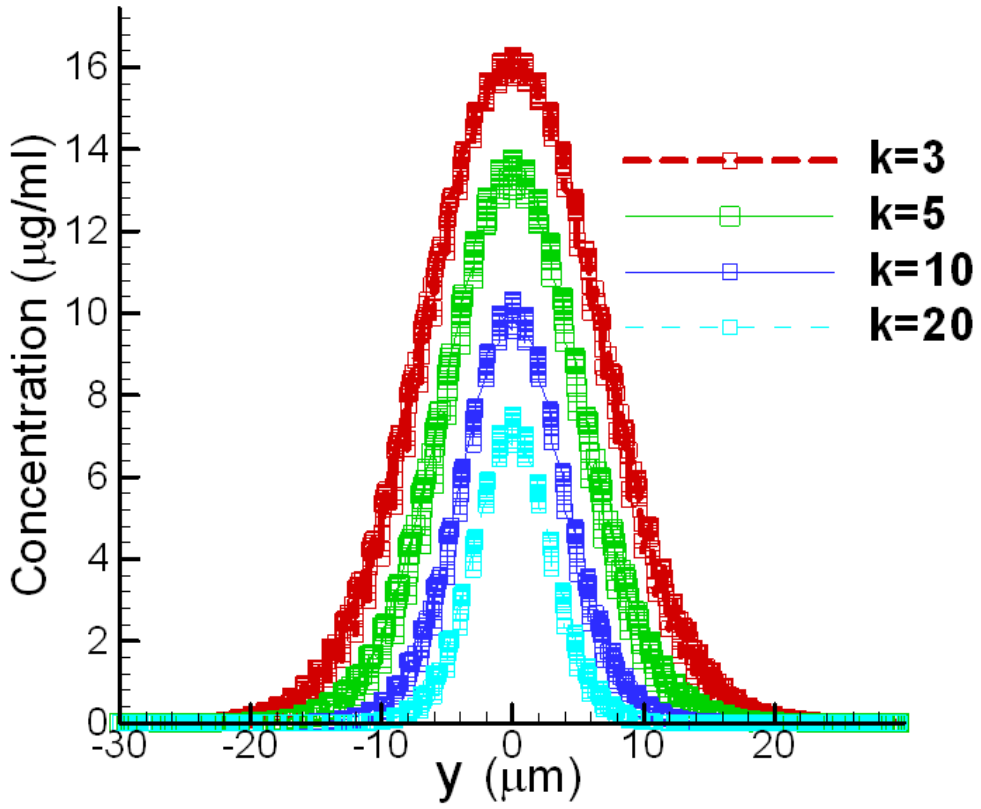
Concentration (μg/ml)
16
14
12
10
8
6
4
2
0
-30
-20
-10
0
10
20
y (μm)
k=3
k=5
k=10
k=20

(b)

Figure 10

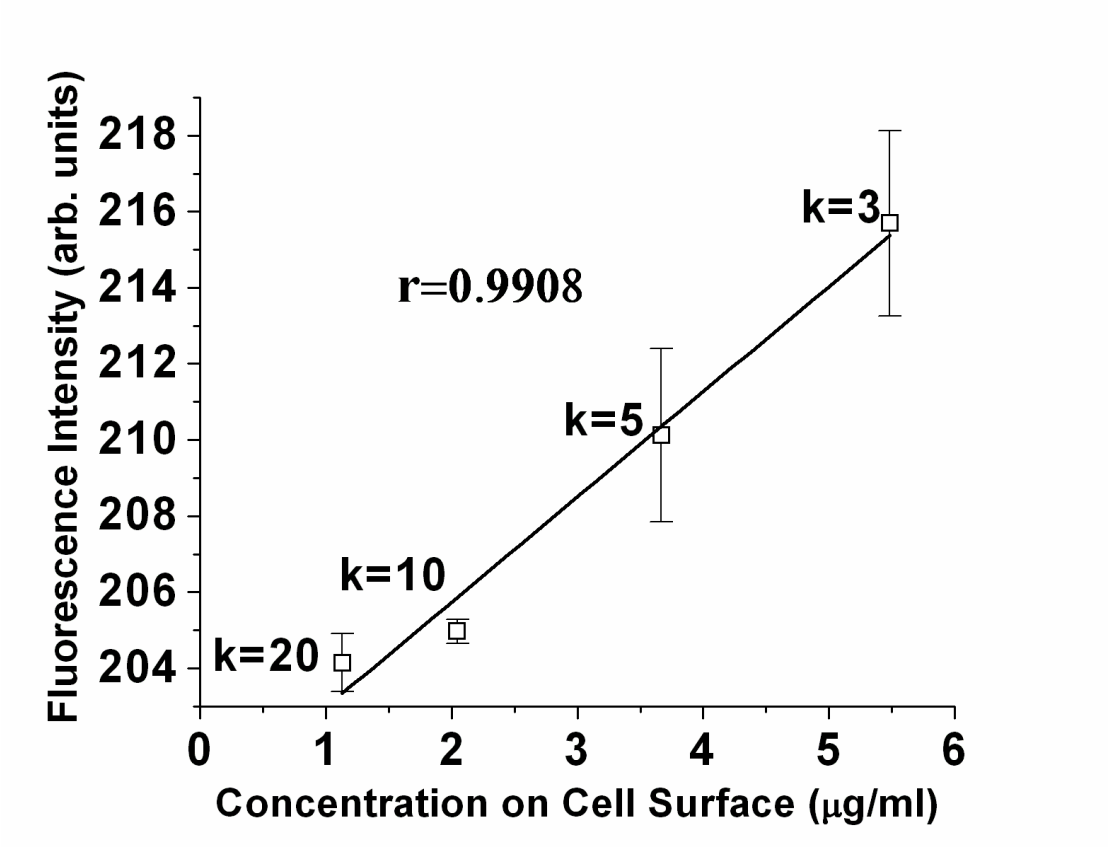
Fluorescence Intensity (arb. units)
218
216
214
212
210
208
206
204
r=0.9908
k=3
k=5
k=10
k=20
0
1
2
3
4
5
6
Concentration on Cell Surface (μg/ml)

Figure 11

TOC graphic